Experimental and numerical analyses of aluminium frames exposed to fire conditions

J. Maljaars [1]

TNO Built Environment and Geosciences, Delft, the Netherlands

F. Soetens [2]

TNO Built Environment and Geosciences, Delft, the Netherlands and

Eindhoven University of Technology, Eindhoven, the Netherlands

Design models are required to assess the behaviour in fire of aluminium structures. These models need to be validated by comparison with test. Up to now tests results are only available for (small scale) individual aluminium components. This paper provides the results of tests carried out on aluminium frames. A finite element model in combination with a sophisticated constitutive model are used to simulate the tests. The results of the simulations agree with that of the tests at room and elevated temperatures.

Keywords: Fire design, fire safety engineering, structural design, creep, elevated temperature

1 Introduction

One of the 'stoppers' for the application of aluminium as structural material for buildings is its sensitivity to fire exposure. Off-shore and marine applications have shown that aluminium alloys can be used for structures with fire risks. However in these cases thick layers of thermal protection material are often required.

Traditionally the fire risk is considered in the design by determining the structural behaviour of individual components – beams, columns, floors – exposed to a standard temperature-time curve. This is a rough approximation of the real behaviour in fire:

---

[1] tel: +31(0)15-2763464, fax: +31(0)15-2763018, e-mail: johan.maljaars@tno.nl

[2] tel: +31(0)15-2763468, fax: +31(0)15-2763018, e-mail: frans.soetens@tno.nl

- On the one hand the standard temperature-time curve does not consider the main influencing fire parameters for the fire temperature – such as the characteristics and amount of combustible material and the sizes of windows.
- On the other hand the individual component assessment does not account for changing distribution of forces in a fire exposed structure due to thermal expansion and weakening of heavily exposed parts.

The natural fire safety concept is a method that provides a more realistic approximation of the fire temperature because it considers the main influencing fire parameters [1], [2]. This concept is incorporated in the design standard EN 1991-1-2 [3]. The more realistic fire temperature approximation should be combined with a more realistic assessment of the structure. This means that the structure should be assessed as a whole or that parts of the structure should be assessed. In the latter case the parts should be selected such that they have negligible interaction with the rest of the structure. This method is known as fire safety engineering (Fig. 1). The possibilities of structural aluminium can be enhanced in a number of applications when applying fire safety engineering [4]. Examples are buildings with a low fire load and large openings such as halls for train stations. EN 1999-1-2 [5] allows to apply the fire safety engineering concept – provided that the assessment is based on proper models that are validated by relevant tests.

Recently a constitutive model is developed for aluminium alloys exposed to fire conditions [6]. This model is based on the results of uniaxial tensile tests. The model is implemented in the finite element software DIANA vs. 9.2 [7]. However this model still needs to be

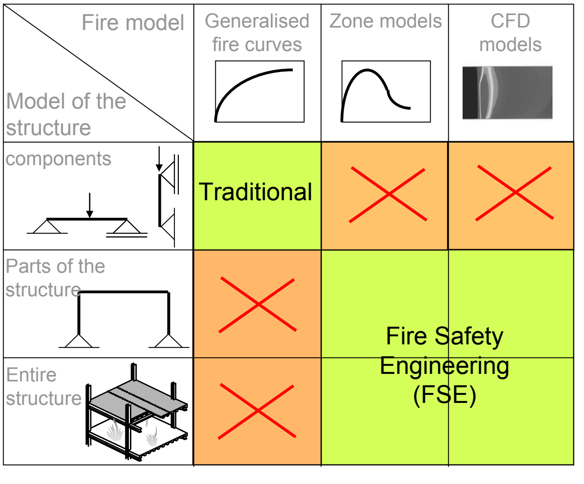

Figure 1. Concepts in a fire design

validated for usage in simulations of structural behaviour. A limited number of test series suited for validation purposes have been found in literature. These test series all comprise individual components such as small scale models of columns [8] and limited numbers of tests on real-scale columns [9], [10] and shear panels [11]. The model is partly validated using these tests [12], [13]. Tests on complete structures or separated parts of structures have not been found in literature. However they are essential for validation of models regarding the influence of thermal expansion and weakening on the resistance of the structure.
For this purpose, tests on aluminium frames are carried out in order to obtain useful validation data. These tests are used to validate finite element models that make use of the constitutive model. This paper describes the results of the tests and the validation.

2 Lay-out of the frames considered

The original plan was to test frames that consist of two aisles (Fig. 2a). However tests at elevated temperatures are expensive – especially when they are large and complicated. For

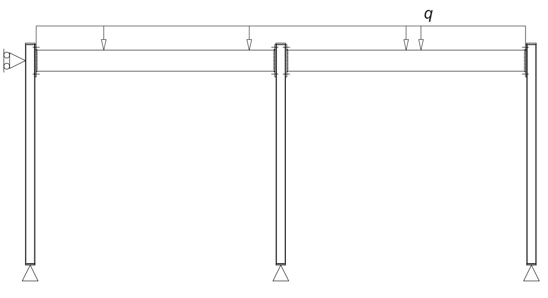

a) Original plan

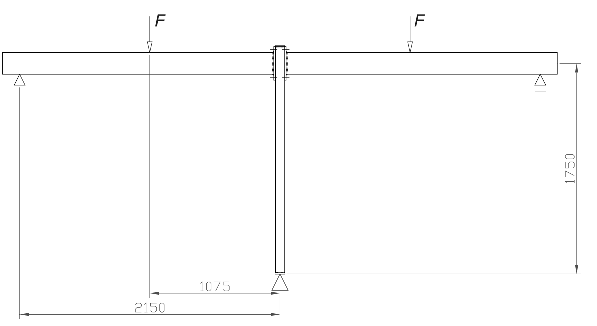

b) Final set-up

Figure 2. Schematic lay-out of the frames (dimensions in mm)

this reason the frames that were finally tested were a simplified representation of the aisles (Fig. 2b). Thermal expansion of the column results in additional bending moments in the beams and the connections between beams and columns. Additionally failure of the frames occurs only after the development of two plastic hinges in the beams – one below the load and one at the connection (Sections 3 and 4 of this paper). Thus the selected frame includes the desired interaction of members and thermal expansion influence.
The selected sections for the column and for the beams are an extruded I-shaped section and an extruded square hollow section respectively (Fig. 3a) – dimensions are measured values. Both sections are composed of alloy 6060-T66. End plates are used for the joint between the column and the beams (Fig. 3b). The end plate is made of alloy 5083-O/H111. Steel bolts grade 8.8 were used in the joints.

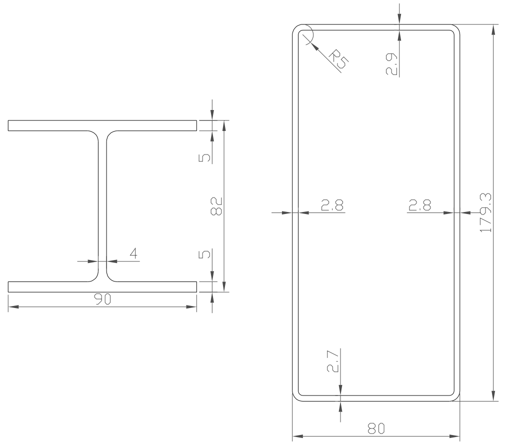

a) Section cross-sections

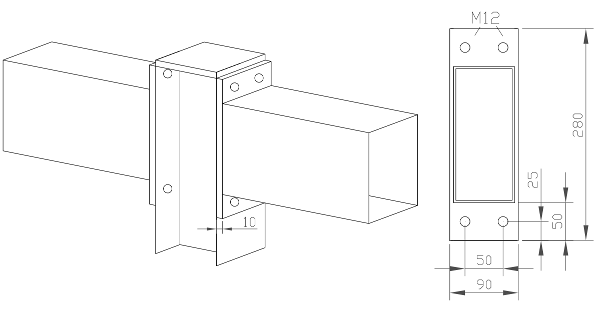

b) Connection between column and beams

Figure 3. Details of the frame (dimensions in mm)

3 Testing

3.1 Tests at room temperature

Two tests were carried out at room temperature in the laboratory of the Centre of Mechanical Structures at TNO, The Netherlands. These tests were carried out upside down (Fig. 4). Hinges and rolls were created using bearings. A stiff steel plate 100 mm x 100 mm x 20 mm was used between the actuator and the specimen as load introduction. The material properties are taken from earlier tests – on the same alloys but on different

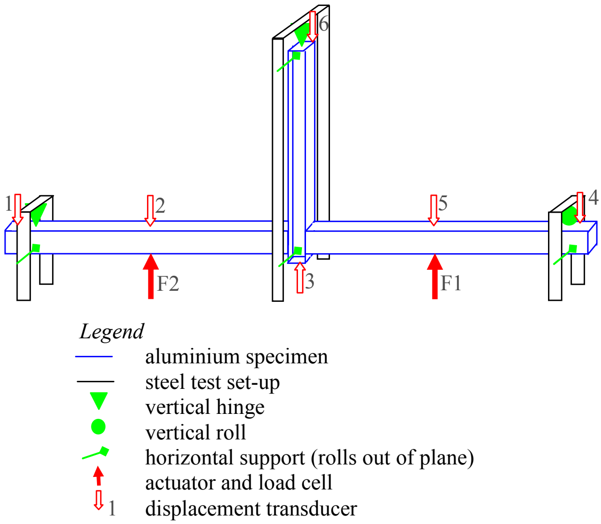

a) Schematic set-up

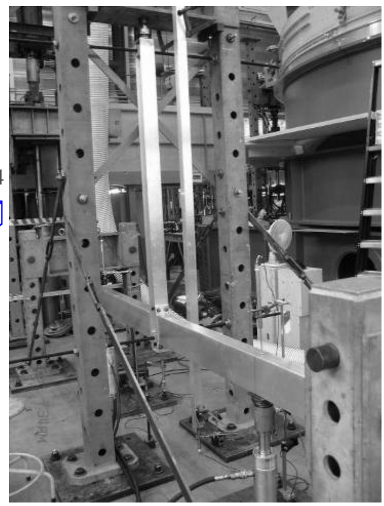

b) Actual set-up

Figure 4. Test set-up at room temperature

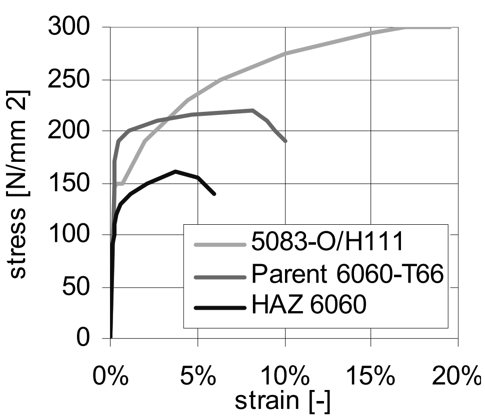

alloy	E [N/mm^2]	$f_{0,2}$ [N/mm^2]	f_u [N/mm^2]
5083-O/H111	71000	152	298
parent 6060-T66	69000	190	220
HAZ 6060	69000	120	160

Figure 5. Constitutive properties at room temperature

batches. Data are provided in Figure 5. Figure 6 presents the failure mode of the test at room temperature. In both tests local buckling of the beam at the load introduction was first observed followed by large deformations of the end plate and finally rupture of the heat affected zone. In Figure 7 the force *F* (at one actuator) is presented as a function of the vertical deflection of the beam at the point of load application. The failure load of the first test was 26.8 kN. For the second test this was 28.5 kN.

3.2 *Tests at elevated temperature*

Three tests at elevated temperature were carried out in normal position – i.e. not upside down. The tests were conducted at the laboratory of Efectis, the Netherlands. Insulation blocks of foam concrete were applied on top of the beams. The blocks are attached to the beams by brackets (Fig. 8). These brackets are not tight so that they do not contribute to

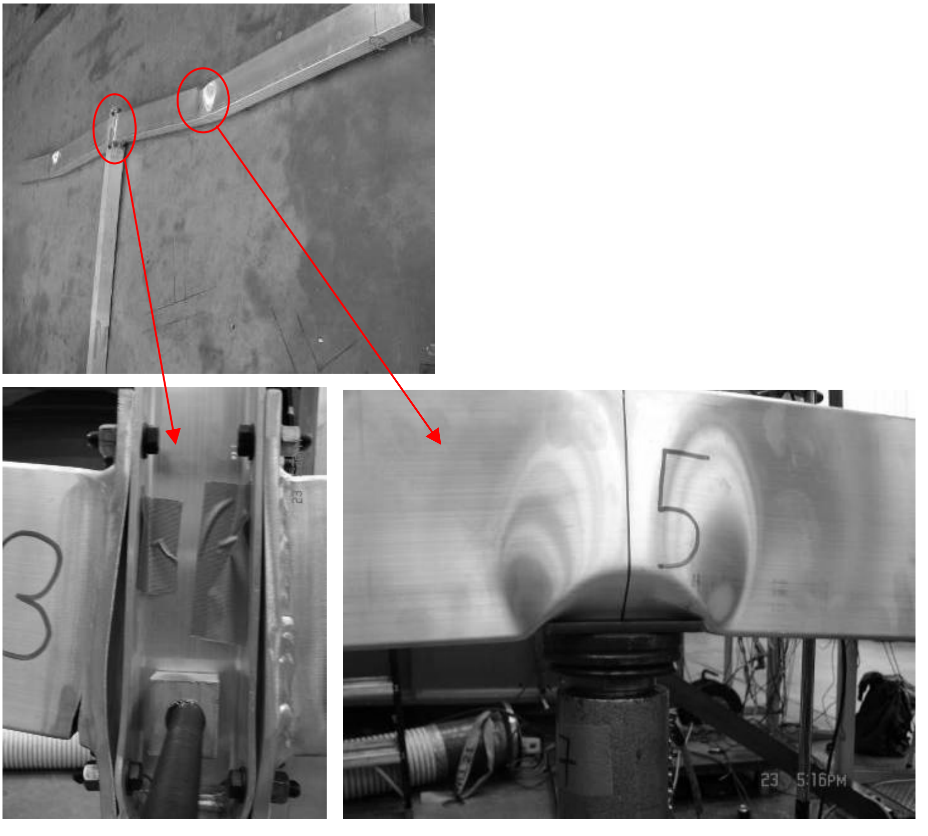

Figure 6. Failure mode of one of the tests at room temperature

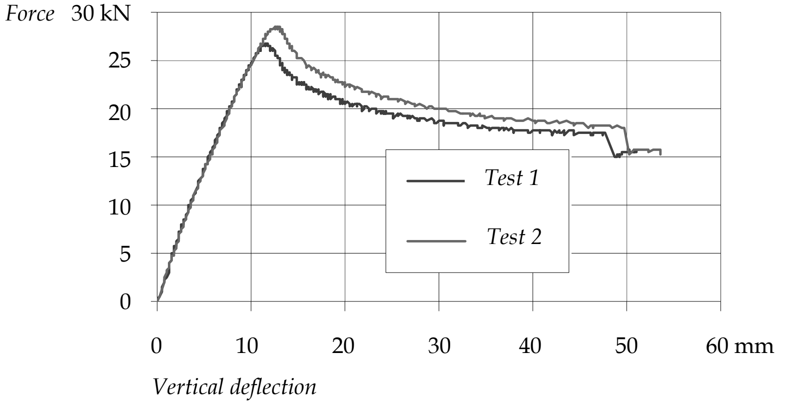

Figure 7. Force deflection diagram of the tests at room temperature

the stiffness of the beams. The insulation blocks form a flexible part of the roof of the furnace. Deformations were measured at the load application points. In total 30 thermocouples were applied on each specimen in order to determine the temperature

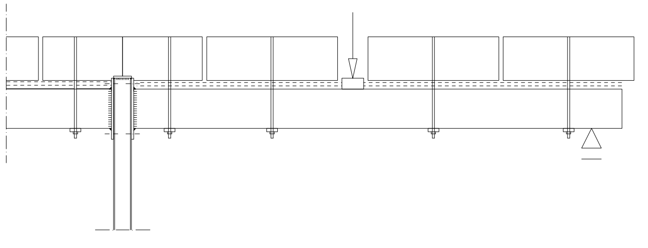

Figure 8. Insulation on top of the specimens for the tests at elevated temperature

distribution along the span and the height of the members. The tests were carried out with a more or less constant load in time and with an increasing temperature in time until the moment of collapse. The collapse temperature was almost equal for all tests. As the loads and deformations were measured more accurately in the 3rd test, the graphs in this paper refer to this 3rd test.

The loads applied were kept at approximately F = 12.5 kN (equal to 45 % of the ultimate resistance of at room temperature). Near the end of the test – when large deformations occurred – it was no longer possible to keep the loads constant. The loads in the 3rd test are presented in Figure 9.

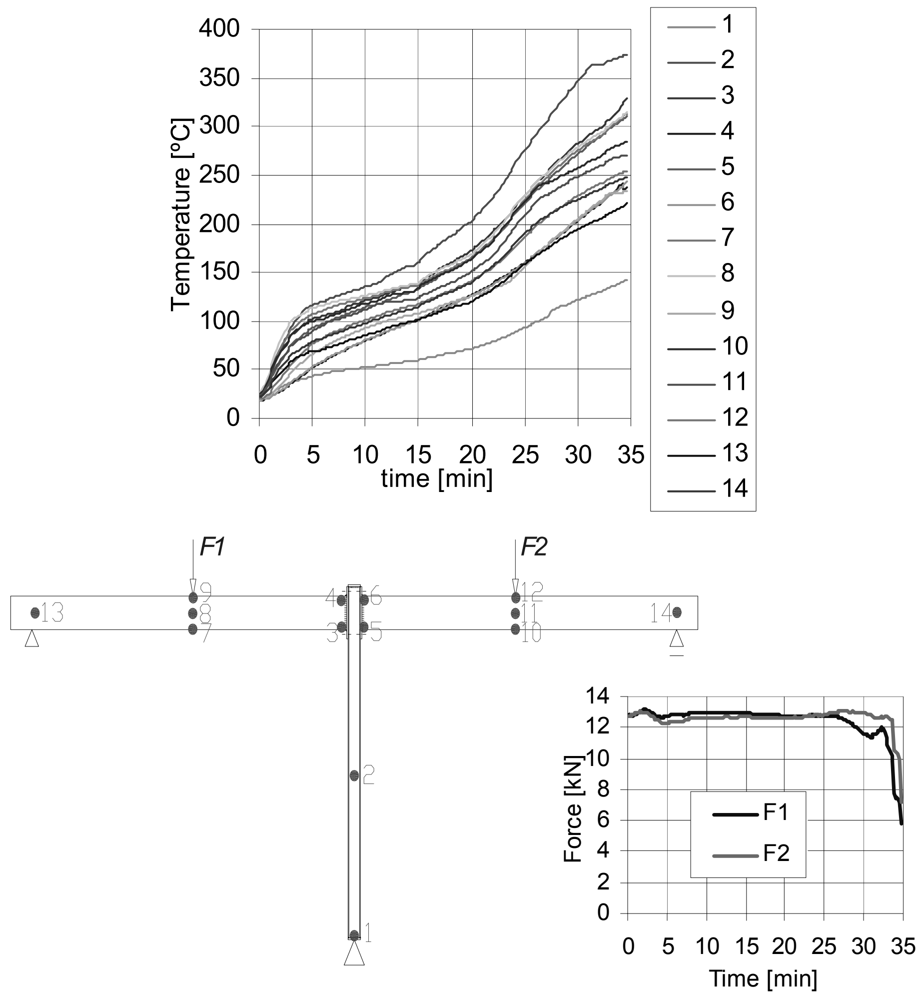

Figure 9. Load and temperature in the 3rd test at elevated temperature

Aluminium members usually need to be protected in order to satisfy the required fire resistance. Only in case of non-severe design fires – e.g. for buildings with a low fire density – the temperature is so low that protection may possibly not be required. In the tests insulation was not applied in order to be able to observe the deformations of the members. Instead the gas temperature was controlled such that it represents the heat flux of an insulated aluminium frame. The heating rate applied was approximately 10 °C/min. Figure 9 presents the temperatures of some important points of the 3rd test. The column foot remains coldest and the column at midspan has the highest temperature. The beams have a temperature in between where the temperature is slightly higher at the bottom flange compared to the top flange.

The material properties are based on a constitutive model that explicitly accounts for creep effects. This model is described in [6]. The parameters of the model are based on earlier tests – on the same alloys but on different batches. Stress strain curves are derived from this model for a constant stress and for a constant heating rate during 30 minutes of fire exposure. These curves are presented in Figure 10. At high-enough temperatures the difference in constitutive properties between the parent metal and the heat affected zone disappears. Therefore the curves at temperatures higher than 250 °C in Figure 10 are considered as representative also for the heat affected zone. Values for the 0.2 % proof stress and the modulus of elasticity are provided in [4].

During the tests the deformation increased exponentially. After 32 minutes the run-away-temperature was reached in the 3rd test which is considered as failure of the frame (Fig. 11). Figure 12 presents the deformations after the test. The deformation shape is

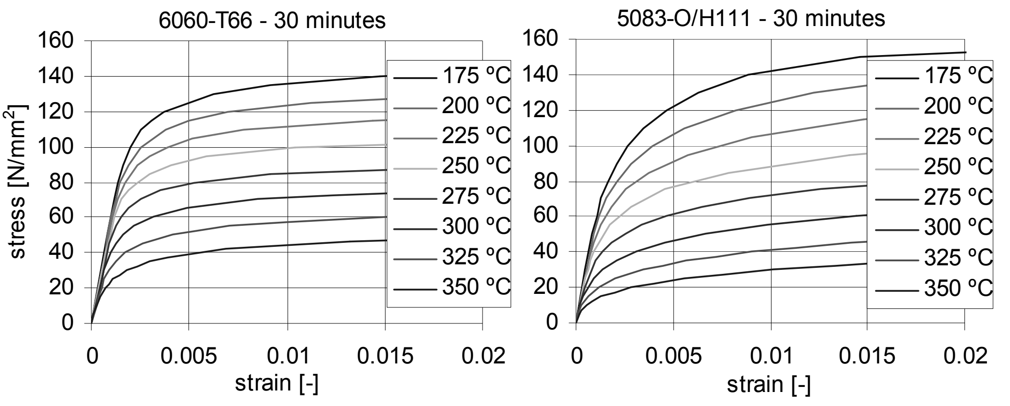

Figure 10. Constitutive properties at elevated temperature

approximately equal to that at room temperature, however the deformations of one beam are considerably larger than that of the other beam (discussed hereafter). The maximum beam temperature at failure was 300-310 ºC. All three tests had the same deformation shape and failure temperature.

3.3 *Discussion of the tests results*

The failure mode of all tests at room and at elevated temperature consisted of local buckling of the beams at load introduction and plastic deformations in the connections followed by rupture of the heat affected zone. The load-displacement and temperature-

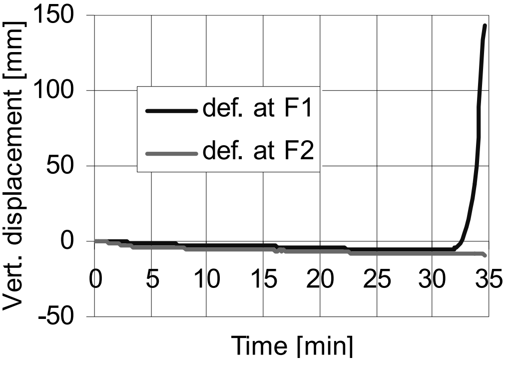

Figure 11. Deformation at load point F1 *in the 3rd test at elevated temperature*

Figure 12. Deformed specimen after the 3rd test at elevated temperature

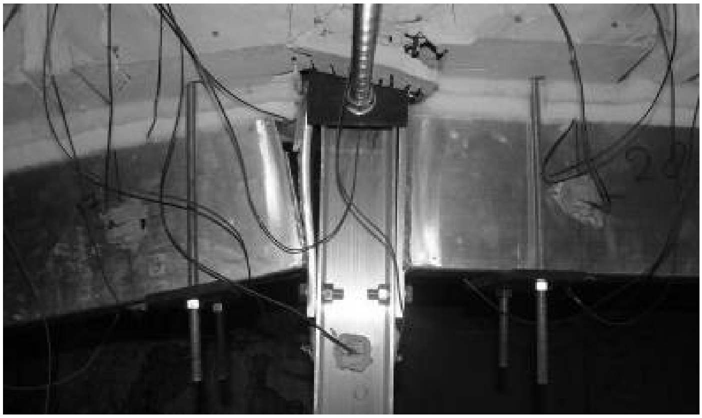

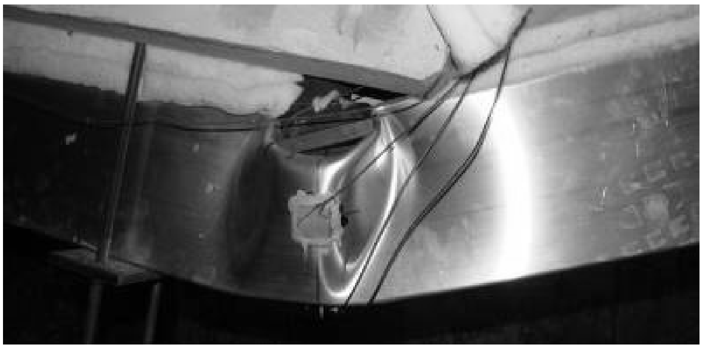

Figure 12. Continued

displacement diagrams of the repeated tests were similar. Based on this it is concluded that the tests are reproducible with reasonable accuracy. Small differences in the ultimate resistance at room temperature are attributed to small differences in geometry such as initial imperfections.

Both tests at room temperature showed a sharp peak in the load-deformation diagram occurring at relatively small plastic deformation. This is typical for failure by local buckling. Small plastic deformations were visible in the joint between beam and column at maximum loading. When these small plastic deformations are compared to tests carried out on T-stubs, [14], it appears that the maximum resistance of the connections is not yet reached at maximum loading of the frame. Based on the deformations it is concluded that failure occurred due to local buckling of the beam at load introduction and that the ultimate resistance was influenced by the non-linear rotation stiffness of the connection.

In the tests at elevated temperature, the temperature at midspan of the column was considerably higher than the temperature of the beams. Figure 10 indicates that the material properties are highly sensitive to temperature. Yet failure of the structure is clearly caused by failure of one of the beams. Hand calculations confirm that the resistance of the column is larger than that of the beams. The fact that only one of the two beams of each frame failed at elevated temperature (Fig. 12) while both beams failed at room temperature (Fig. 6), is attributed to the small differences in temperature between the beams in the tests at elevated temperature. The temperature of the beam that failed was approximately 10 °C higher than that of the other beam. This results in lower values for the material strength and stiffness for the beam that failed. Thermal expansion of the column introduces a compression force in the column and additional bending moments in the joints.

4 Finite element simulations

4.1 Finite element model

Since the column was not subjected to flexural buckling and since the loads and geometry are symmetrical about the column axis only one half of the structure is modelled in the finite element program DIANA 9.2. The model is shown in Figure 13. It consists of 8-noded, curved shell elements CQ40S with 7 integration points through thickness and with mesh refinements in the load introduction area and joint area. Interface elements CQ48I are applied at the joint between the end plate and the column wall. These interface elements have a negligible stiffness for tension ($E/10000$) and a very high stiffness for compression ($E\times10000$) in order to simulate that the end plate can be pulled of the column but cannot penetrate the column. The bolts are not modelled. Instead the nodes in the column flange at the position of the bolts are tied with the corresponding nodes in the end plates.
Special attention was paid to the modelling of the load introduction (Fig. 14). While the corners of the beam section in reality are rounded the model uses straight corners. The contact plane is between the edges of the rounded off corners. Load introduction is modelled by reducing the load introduction plate in the model to such an extent that the contact plane area is equal as well as the distance between the section webs and the edge of the contact plane. Again interface elements are applied between the load introduction plate and the beam upper flange with negligible stiffness for tension and very high stiffness for compression.

4.2 *Simulation of tests at room temperature*

The constitutive properties according to Figure 5 are implemented in the model and the dimensions are modelled as measured. The load-displacement diagram resulting from the simulation is compared with that of the tests in Figure 15a. The simulated behaviour is similar to the test results. The ultimate load in the simulations is slightly lower. This is attributed to friction between the steel plate and the beam at the load introduction – which is not modelled – and to differences in material properties between different batches of the same alloys. The difference in ultimate resistance between the simulations and the tests is 7% for the first test and 11% for the second test. This is considered as accurately enough for the purpose of this research in which the focus is on elevated temperatures. The deformation pattern of the simulation (Fig. 15b) agrees well with that in the tests (Fig. 6).

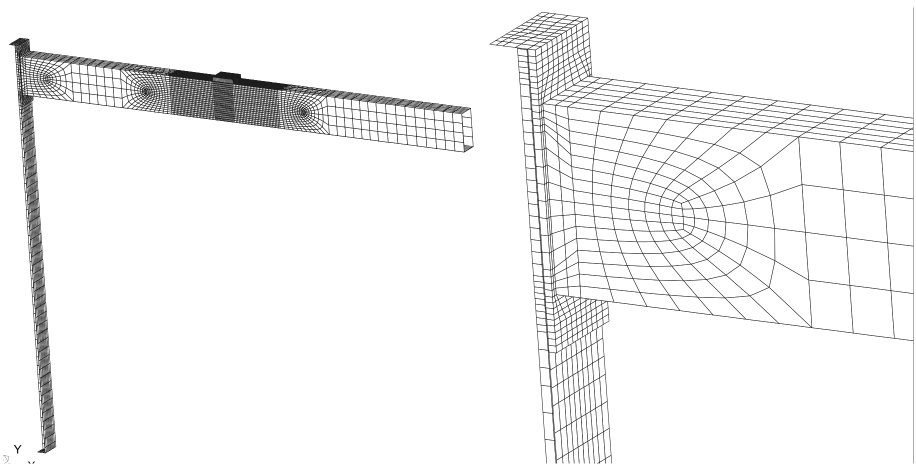

Figure 13. Finite element model

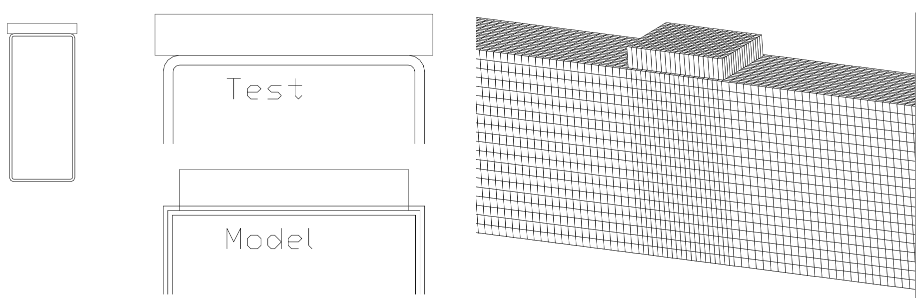

Figure 14. Load introduction in the finite element model

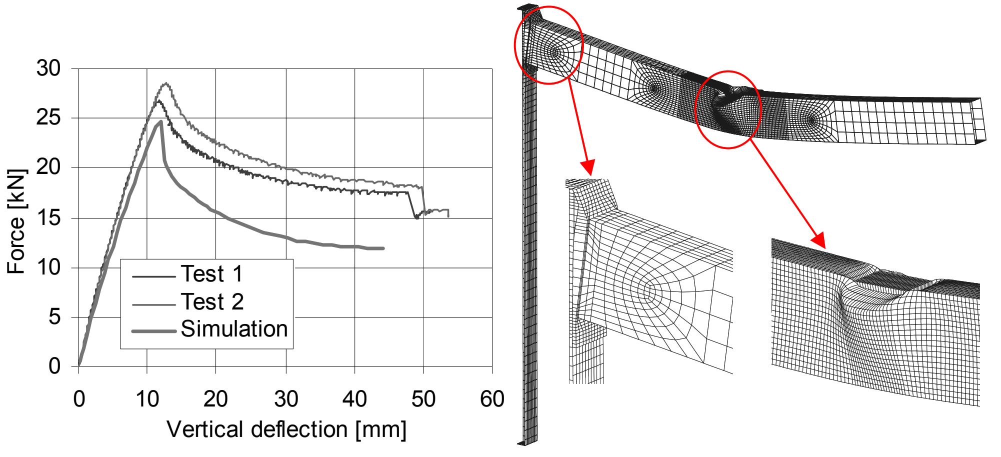

a) Force-deflection diagram *b) Deformations*

Figure 15. Results of the simulation at room temperature

4.3 *Simulation of tests at elevated temperature*

The constitutive properties according to Figure 10 are implemented in the model and the dimensions are modelled as measured. Measured heating rates including thermal gradients are also modelled (Fig. 16b). Figure 16a shows the deformation as a function of time for the test and the simulation. The simulated deformation pattern is similar to that at room temperature (Fig. 15b).

Comparing the two graphs in Figure 16a, it appears that the failure time is predicted accurately. The deformations during the first stage of testing – before the occurrence of the run away temperature – do not agree. However this is attributed to the fact that the displacement sensor was heated during the test. This causes the measured displacement to be inaccurate.

5 Conclusions

- Fire Safety Engineering (FSE) provides a more accurate approximation of the real behaviour in fire as compared to a traditional fire design. Due to the sensitivity of aluminium for fire conditions, a realistic – not too conservative – approximation of the real behaviour is often required in order to be a realistic alternative as structural material. For this reason FSE is an excellent method to evaluate the fire resistance of aluminium structures.

- A test programme consisting of frames at room temperature and at fire conditions has been conducted. The resistance of the selected frames at elevated temperature depends on the interaction between failure mechanisms and on the influence of thermal expansion. This has resulted in valuable data for verification of structural models to be used in fire safety engineering. Such verification is essential for a sound fire safety engineering approach.
- A finite element model was created of the tested frames. The model is able to predict the ultimate resistance at room temperature with reasonable accuracy (difference 7-11 %). The small difference can be well explained by simplifications applied in the model. For simulations at elevated temperature a previously developed constitutive model is used. The finite element model is well able to predict the run-away temperature of the tests at fire conditions (difference 3%). Thus the combination of the constitutive model and the finite element model results in a powerful tool to be used in fire safety engineering of aluminium structures.

Acknowledgements

The members of the joint-industry project group 'Fire Design of Aluminium Structures', The Netherlands, are kindly acknowledged for their contribution.

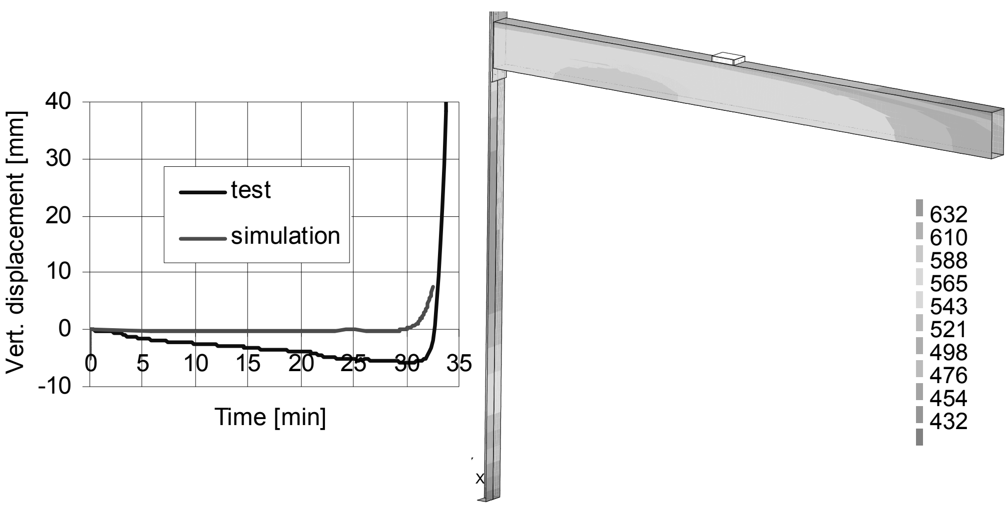

a) Deformation as a function of time *b) Modelled temperature [°K] after 32 min.*

Figure 16. Simulation at elevated temperature

References

[1] J.C. Dotreppe, C. Hahn, B.A. Haseltine, M. Kersken-Bradley, L. Krampf, J. Kruppa, M. Law, J. Mathez, E. Pedersen, P. Schaumann, J.B. Schleich, G. Storti, L. Twilt, Actions on structures exposed to fire, Commission of European Communities, Eurocodes Chapter 20, 1990.

[2] Kruppa, J. Performance-based code in fire resistance: first attempt by Eurocodes, in: Proc. of International conference on performance-based codes and fire safety design method, Ottawa, 1996.

[3] EN 1993-1-2 (2005) Eurocode 3: Design of steel structures – Part 1-2: General Rules – Structural fire design

[4] J. Maljaars, L. Twilt, J.H.H. Fellinger, H.H. Snijder, F. Soetens, Aluminium structures exposed to fire conditions – an overview, *Heron*, Vol. 55 (2010) No. 2, pp. 85-122.

[5] EN 1999-1-2 (2007) Eurocode 9: Design of aluminium structures – Part 1-2: General Rules – Structural fire design

[6] J. Maljaars, F. Soetens, L. Katgerman, Constitutive model for Aluminum Alloys Exposed to Fire Conditions, Metallurgical and Materials Transactions A, 39 (2008), pp. 778-789

[7] F.C. de Witte, W.P. Kikstra DIANA users manual – release 9.2, TNO Diana, Delft, 2007.

[8] J. Maljaars, F. Soetens, H.H. Snijder, Local buckling of aluminium structures exposed to fire. Part 1: tests, *Thin Walled Structures*, 47 (2009), pp.1404-1417

[9] N.K. Langhelle, Experimental validation and calibration of nonlinear finite element models for use in design of aluminium structures exposed to fire, Norwegian University of Science and Technology, Trondheim, 1999

[10] N.K. Langhelle, E. Eberg, J. Amdahl, S. Lundberg, Buckling tests of aluminium columns at elevated temperatures, in: Proc. of 15th OMAE, Firenze, 1996

[11] J. Amdahl, N.K. Langhelle, S. Lundberg, Aluminium Plated Structures at Elevated Temperatures, in: Proc. of 20th OMAE, Rio de Janeiro, 2001

[12] J. Maljaars, L. Twilt, F. Soetens, F. Flexural buckling of fire exposed aluminium columns, *Fire Safety J.*, 44 (2009), pp. 711–717

[13] J. Maljaars, F. Soetens, H.H. Snijder, Local buckling of aluminium structures exposed to fire. Part 2: finite element models, *Thin Walled Structures*, 47 (2009), pp. 1428-1428

[14] G. De Matteis, A. Mandara, F.M. Mazzolani, T-stub aluminium joints: the infulence of behavioural parameters, *Computers and Structures*, 78 (2000), pp. 311-327